Journal of Applied Polymer Science

Influence of structure of amines on the properties of amines-modified reduced graphene oxide/polyimide composites

Lang Ma,[1] Guojian Wang,[1,2] Jinfeng Dai[1]
[1]School of Materials Science and Engineering, Tongji University, Shanghai, 201804, China
[2]Key Laboratory of Advanced Civil Engineering Materials, Ministry of Education, Shanghai, 201804, China
Correspondence to: G. Wang (E-mail: wanggj@tongji.edu.cn)

ABSTRACT: Graphene oxide (GO), as an important precursor of graphene, was functionalized using alkyl-amines with different structure and then reduced to prepare reduced amines grafted graphene oxide (RAGOs) by $N_2H_4 \cdot H_2O$. The successful chemical amidation reaction between amine groups of alkyl-amines and carboxyl groups of GO was confirmed by Fourier transform infrared (FTIR), X-ray photoelectron spectroscopy (XPS), and thermal gravimetric analysis (TGA). Then RAGOs/polyimide nanocomposites were prepared via *in situ* polymerization and thermal curing process with different loadings of RAGOs. The modification of amine chains lead to homogenous dispersion of RAGOs in the composites and it formed strong interfacial adhesion between RAGOs and the polymer matrix. The mechanical and electrical properties of polyimide (PI) were significantly improved by incorporation of a small amount of RAGOs, the influence of structure of amines grafted on RAGOs on the enhancement effects of composites was discussed. The research results indicated that the proper structure of amine could effectively enhance the properties of composites. © 2016 Wiley Periodicals, Inc. J. Appl. Polym. Sci. **2016**, *133*, 43820.

KEYWORDS: composites; graphene; mechanical properties; polyimides

Received 23 December 2015; accepted 25 April 2016
DOI: 10.1002/app.43820

INTRODUCTION

Polymer composites with carbon-based nano-fillers have drawn widely scientific and industrial attention, since its significant improvement of valuable properties of the composites and less sacrifice of the process ability of polymers.[1–4] Among the carbon-based nano-fillers, graphene has generated much interest all over the world due to its unique structure and properties.[5–7] Graphene has the potential to reinforce mechanical, thermal, and electrical properties of various polymers in many applications, there have been many reports on this subject.[8–10] However, it has high surface area and weak interfacial adhesion with polymer matrix because of its relative inert surface. This makes the dispersed graphene tends to re-aggregate. The re-aggregated graphene could not show its extraordinary properties, resulting in the very limited improvement effect. And the weak filler–matrix interfacial interactions could not well transfer the stress. This unsolved critical issues have limited the practical applications of graphene in polymers.

Graphene oxide (GO), as an important precursor of graphene, is usually obtained by modified Hummers method in a low cost way. There are plenty of oxygen-containing groups on its surface and edges, such as hydroxyl, epoxy, carbonyl groups, and so on.[11–13] The existence of these oxygen-containing groups provides versatile sites for further chemical modification of GO. Among the modification method, the formation of covalent bond between GO and target grafted chains could make the chains stick to the surface or edges of GO tightly. The introduction of the grafted chains could not only hinder the aggregation of GO,[14,15] but also contribute to the formation of strong interface interactions between the nano-fillers and polymer matrix, resulting in the dispersion stability of the nano-fillers.[16] Moreover, the further removal of the residual unreacted oxygen-containing groups in GO during the reduction process would make its chemical structure more complete. It could minimize the defects of graphene to achieve better properties and more excellent enhancement effect.

In this work, GO was prepared by modified Hummers method[17,18] and then covalently modification by adopting four types of amines with different numbers of functional groups and chain lengths: ethylene-diamine (EDA), hexa-methylene-diamine (HMDA), dodecyl-amine (DCA), and n-octadecyl-amine (ODA). By the modification of the different amine chains, the re-aggregation of rGO (reduced graphene oxide) was inhibited; the more uniform dispersion of the nano-fillers on the polymer matrix could favor the enhancement effect. What's more, with the introduction of the amine chains onto the

surface of rGO, the filler–matrix interfacial interactions were improved, better stress transferring, and more excellent mechanical properties were achieved. The different chain lengths and functional groups of the amines showed different behaviors in the composites, which would contribute the better understanding of functionalization of graphene with different amine chains and functional groups. Subsequently, the amines grafted GOs were reduced by hydrazine hydrate ($N_2H_4 \cdot H_2O$) to produce reduced amines grafted GOs (RAGOs). After that, different loadings of RAGOs were introduced to polyimide (PI) via *in situ* polymerization and thermal curing process to prepare composites. The effect of different amine chains on the properties of PI were investigated and compared with each other. The results indicated that there was a well dispersion of RAGOs in the polymer matrix, forming strong interfacial combination between RAGOs and the polymer matrix. The introduction of RAGOs could significantly improve the properties of PI films.

EXPERIMENTAL

Materials

Graphite flakes (≈48 μm in diameter, purity of 98%) were purchased from Qingdao Yifan Company, China; 4,4′-oxydianiline (CP), pyromellitic dianhydride (PMDA, CP), *N*,*N*-dimethylformamide (DMF, AR), concentrated sulfuric acid (H_2SO_4, 98%, CP), hydrogen peroxide (H_2O_2, 30%, AR), sodium nitrate ($NaNO_3$, AR), hydrazine hydrate($N_2H_4 \cdot H_2O$, AR), ammonium hydroxide ($NH_3 \cdot H_2O$, AR), potassium permanganate ($KMnO_4$, AR), hydrochloric acid (HCl, 36%, CP), ethyl alcohol (EtOH, AR), thionyl chloride ($SOCl_2$, AR), ethylene-diamine (EDA, AR), hexa-methylene-diamine (HMDA, AR), dodecyl-amine (DCA,CR), and n-octadecyl-amine (ODA, AR) were supplied by Sinopharm Chemical Reagent Co, Ltd, China.

Preparation of RAGOS

GO was prepared by a modified Hummers method reported elsewhere.[17,18] For the preparation of RAGOs, a total of 400 mg dried GO powder was dispersed in 100 mL $SOCl_2$ by ultrasonication for 2 h and the suspension was then refluxed at 70 °C for 24 h in the presence of 1 mL DMF to obtain GO-Cl. A total of 500 mg different amines (EDA, HMDA, DCA, or ODA) were dissolved in 30 mL EtOH respectively to obtained solutions. About 100 mg GO-Cl powder was then added, respectively, to amine/EtOH solutions and the suspension was dispersed using sonication for 2 h at 70 °C. Then the suspension was filtered and the filter cake was washed with EtOH to remove excess amines. Finally the filter cake was dried by vacuum freeze-drying, the amine grafted GOs (GO-As) were obtained.

GO-As were reduced by $N_2H_4 \cdot H_2O$ to get RAGOs. Typically, the each GO-As was dispersed in DMF (1 mg/mL) with ultrasonic treatment and then $NH_3 \cdot H_2O$ was added to regulate the pH to about 9. After that, $N_2H_4 \cdot H_2O$ (1 mL) was added into the suspension (100 mL), the mixture was refluxed at 95 °C for 2 h. Finally, after filtration and washing with EtOH, different RAGOs were obtained by vacuum freeze-drying and labeled as rGO-EDA, rGO-HMDA, rGO-DCA, and rGO-ODA according to the different amines. For the purpose of comparison, reduced graphene oxide (rGO) was prepared by the reduction of GO with $N_2H_4 \cdot H_2O$, the reduction procedure was same as the GO-As reduction to RAGOs.

Preparation of PI and RAGOS/PI Composites

Preparation of PI. To prepare PI, 2.0023 g (10 mmol) 4,4′-oxydianiline was firstly dissolved in 25 mL of DMF in a three-necked flask equipped with a mechanical stirrer and nitrogen inlet and outlet at room temperature. Then 2.1856 g (10.02 mmol) PMDA was added in batches. After the PMDA was completely dissolved, the mixture was stirred under nitrogen atmosphere for 24 h at room temperature, a viscous polyamic acid (PAA) solution was produced.

PAA was casted on a glass plane and treated under 80 °C for 2 h to evaporate the solvent. Then the temperature was increased from 80 to 300 °C with a rate of 3 °C/min. During this course, it was maintained at 100, 150, 200, 250, and 300 °C for 30 min each. Finally, PI film was obtained.

Preparation of RAGOs/PI Composites via *In Situ* Polymerization

For the preparation of PI composites with different loadings of RAGOs (0.1, 0.3, 0.5, and 1.0 wt %) via *in situ* polymerization, a certain amount of RAGOs was firstly dispersed in 25 mL DMF by sonication for 2 h, then 2.0023 g (10 mmol) 4,4′-oxydianiline was added under nitrogen atmosphere at room temperature. After 4,4′-oxydianiline was totally dissolved under stirring, 2.1856 g (10.02 mmol) PMDA was added in batches. The mixture was treated at room temperature under stirring and nitrogen atmosphere for 24 h to produce RAGOs/PAA mixture. The following thermal curing process was the same as the preparation of PI from PAA. For the purpose of comparison, rGO/PI composites were also prepared as the same preparation route as RAGOs/PI composites. Figure 1 showed the scheme of preparation of PI and the composites.

Characterization

Fourier transform infrared (FTIR) spectra were obtained using an EQUINOX55 spectrometer (Bruke Co., Germany) in the range of 4000–600 cm^{-1}. Scanning electron microscopy (SEM) was adopted to observe the samples morphology on a Quanta 200 FEG (FEI Co., The United States) at an accelerating voltage of 15 kV. The samples were sputtered with thin layers of Au. X-ray photoelectron spectroscopy (XPS) measurement was performed by a PHI 5000C ESCA System XPS (Perkin Elmer Co., The United States) with aluminum target, high voltage of 14.0 kV and power of 300 W. Thermal gravimetric analysis (TGA) was conducted on STA449C TGA/DSC analyzer (Netzsch Co., Germany) with a heating rate of 20 °C/min from room temperature to 800 °C under nitrogen atmosphere. The electrical conductivity of the films was measured on Keithley analyzer (4200-SCS, The United States). Mechanical properties of film samples were evaluated using a universal testing machine according to the standard of ASTM-D882 with a speed of 5 mm/min.

RESULTS AND DISCUSSION

Chemical Structure of RAGOS

The existence of oxygen-containing groups, such as hydroxyl and carboxyl and epoxy group on the surface and edges of GO provided the reaction sites with other chemical groups. After

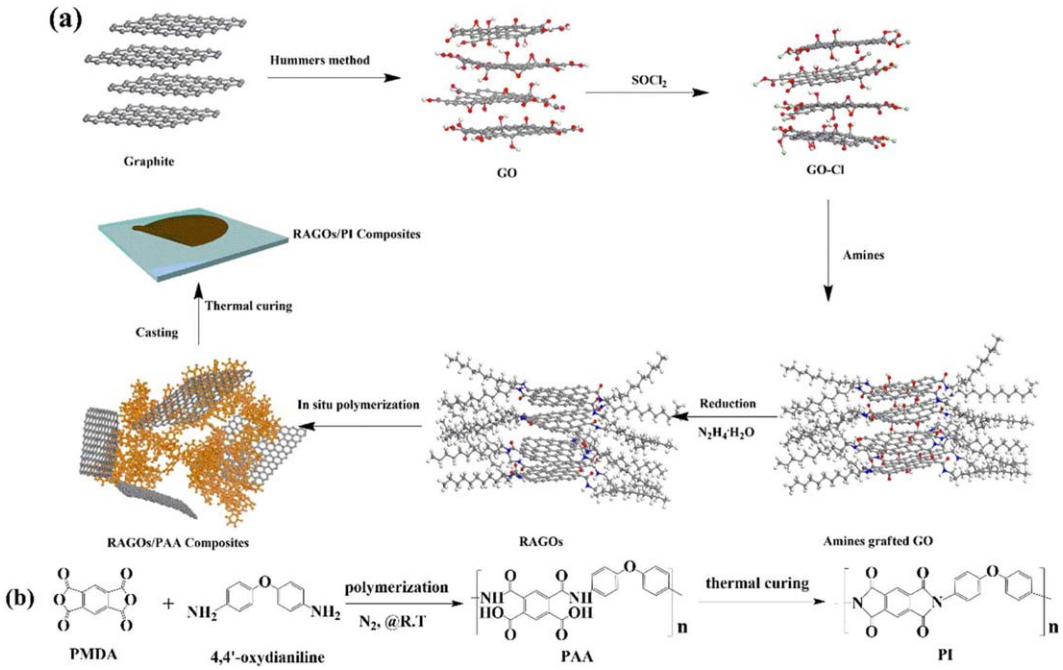

Figure 1. Scheme of preparation of (a) RAGOs and PI composites, (b) neat PI. [Color figure can be viewed in the online issue, which is available at wileyonlinelibrary.com.]

reaction with $SOCl_2$ to form GO-Cl, it could react with amine groups easily. Thus, the amine chains covalently grafted to the surface of GO. Furthermore, by the reduction of $N_2H_4 \cdot H_2O$, most of the residual oxygen-containing groups could be removed from the surface of alkyl-amines grafted GO. The successful grafting of alkyl-amines to the surface of GO was characterized by FTIR, as shown in Figure 2. The pristine GO showed major FTIR absorption peaks at 3200, 1720, 1623, and 1048 cm^{-1}, which were attributed to stretching vibration of the OH group, C═O bond of carbonyl, deformation vibration of the O—H bond and stretching vibration of C—O—C, respectively, indicating its super hydrophilic property. However, in comparison with pristine GO, RAGOs showed totally different FTIR vibrations. The peaks at

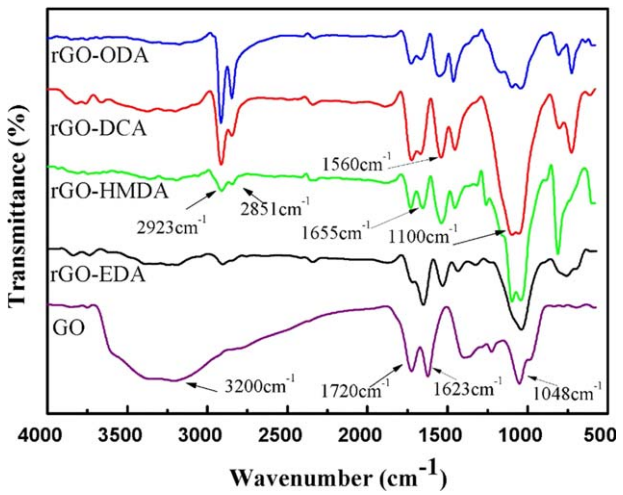

Figure 2. FTIR spectra of GO and RAGOs. [Color figure can be viewed in the online issue, which is available at wileyonlinelibrary.com.]

2923 and 2851 cm^{-1} correspond to the asymmetric and symmetric stretching of —CH_2 group of alkyl-amines, which provided the evidence for the presence of alkyl-amines on GO surface. The appearance of the peaks at 1560 cm^{-1} (N—H deformation vibrations), 1100 cm^{-1} (C—N stretching vibrations), and 1655 cm^{-1} (C═O stretching vibration, amide II) indicated the successful chemical interaction between alkyl-amines and GO with formation of amide linkages.

XPS characterization results were showed in Figure 3 and Table I. The main elements were C, O, and N for the samples. The C and O contents were 66.41 and 33.47% for the pristine GO, the N element was not detected as expected. However, the C content increased and O content decreased significantly for the RAGOs in comparison with GO. The C/O ratios increased from 1.98 of GO to 8.22, 8.18, 8.13, and 8.43 of rGO-EDA, rGO-HMDA, rGO-DCA, and rGO-ODA, respectively. It was attributed to the removal of most of oxygen-containing groups on the surface of GO. And it showed that the molar contents of nitrogen element were 4.98, 5.28, 3.06, and 3.17% for rGO-EDA, rGO-HMDA, rGO-DCA, and rGO-ODA, respectively. Therefore, according to the eq. (1), the weight ratio of N element in the grafted chains were 5.60, 5.91, 3.45, and 3.58% for the rGO-EDA, rGO-HMDA, rGO-DCA, and rGO-ODA, respectively. It provided the evidence for the presence of N on the surface of RAGOs, revealing the successful incorporation of alkyl-amines. Furthermore, the molar contents of N element for rGO-EDA and rGO-HMDA were higher than that of rGO-DCA and rGO-ODA. It was because of the different quantity amine groups on the end of the amine chains for diamine and monoamine. However, the more grafted weight ratio would cause more defects on the surface of graphene, resulting in more destruction on the properties of graphene.

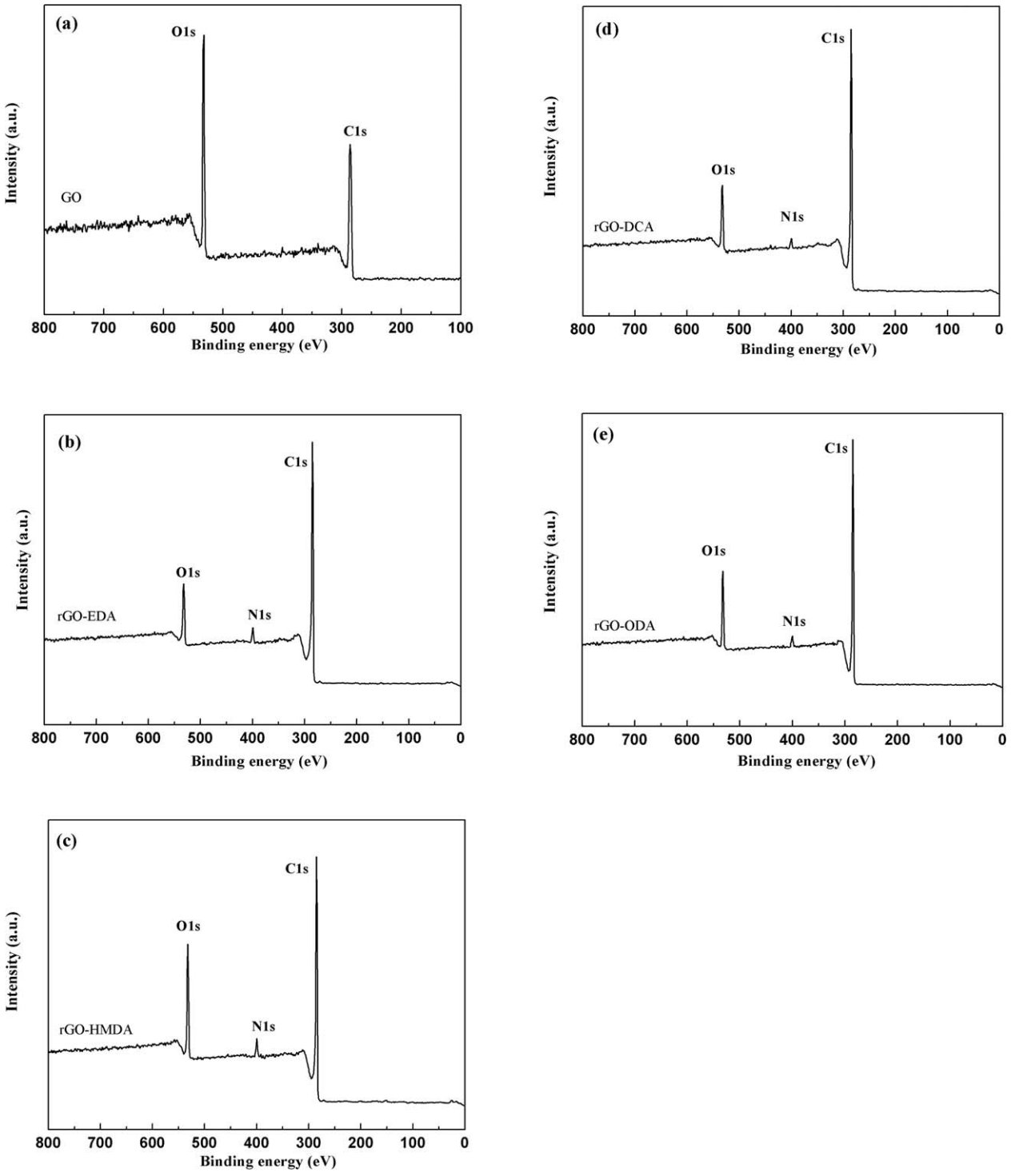

Figure 3. XPS spectra of RAGOs, (a) GO, (b) rGO-EDA, (c) rGO-HMDA, (d) rGO-DCA, and (e) rGO-ODA.

$$w_N = \frac{C_N \times M_N}{C_N \times M_N + C_C \times M_C + C_O \times M_O} \times 100\% \quad (1)$$

Thereinto, w_N represents the weight ratio of N, C_N, C_C, and C_O represent the content of the N, C, and O, M_N, M_C, and M_O represent the molar mass of N, C, and O.

Figure 4 summarized the results of the C1s XPS spectra of RAGOs. The C1s XPS spectra could fit into for components: C—C (284.5 eV) for sp^2 carbon, C—N (285.7 eV), C—O (286.3 eV), and C═O (288.5 eV). The small but dominant peak around 285.7 eV, attributing to C—N, indicated that the

Table I. Element Contents and C/O Ratios of GO and RAGOs

Samples	Atomic content (%)			
	C	O	N	C/O
GO	66.41	33.47	—	1.98
rGO-EDA	84.65	10.03	4.98	8.22
rGO-HMDA	84.35	10.31	5.28	8.18
rGO-DCA	85.74	10.54	3.06	8.13
rGO-ODA	85.95	10.28	3.17	8.43

successful covalently bonding between amines and GO. The most dominant peak at 284.5 eV corresponded to C—C, while the intensity of both C═O and C—O peaks were much lower than that of C—C, revealing that there were only a slight of oxygen-containing groups on the surface of RAGOs. The results were in good accordance with FTIR analysis. Therefore, it could be concluded that the alkyl-amines were covalently bonded to the surface of RAGOs and most of the oxygen-containing groups were removed by the modification of alkyl-amines and reduction of $N_2H_4 \cdot H_2O$.

The thermal decomposition behaviors of GO, rGO, and RAGOs were studied by TGA, the results were shown in Figure 5 and Table II. From Figure 5, it could be seen, for GO, there was a weight loss of about 10% below 100 °C, corresponding to the evaporation of moisture due to its super hydrophilic property. The major loss of about 30% in the temperature range from 150 to 300 °C was associated with thermal decomposition of oxygen-containing groups to yield CO_2 and CO.[19,20] The slight weight loss from 300 to 800 °C mainly corresponded to the thermal decomposition of carbon skeleton and the residual weight finally reached 42.49% at 800 °C, as shown in Table II. While for rGO, it showed rather different thermal behavior. There was only 2.72% weight loss below 100 °C. The residual weight was 93.23% at 300 °C, which was much higher than that of GO, indicating the removal of most of the oxygen-containing groups after reduction. It showed similar thermal degradation from 300 to 800 °C with GO and the residual weight finally reached 84.22% at 800 °C.

Compared with the GO, RAGOs showed much better thermal stability. From Figure 5, it could be seen that RAGOs had slight weight loss before 100 °C, which was much less than GO, showing similar thermal degradation as rGO. It indicated the

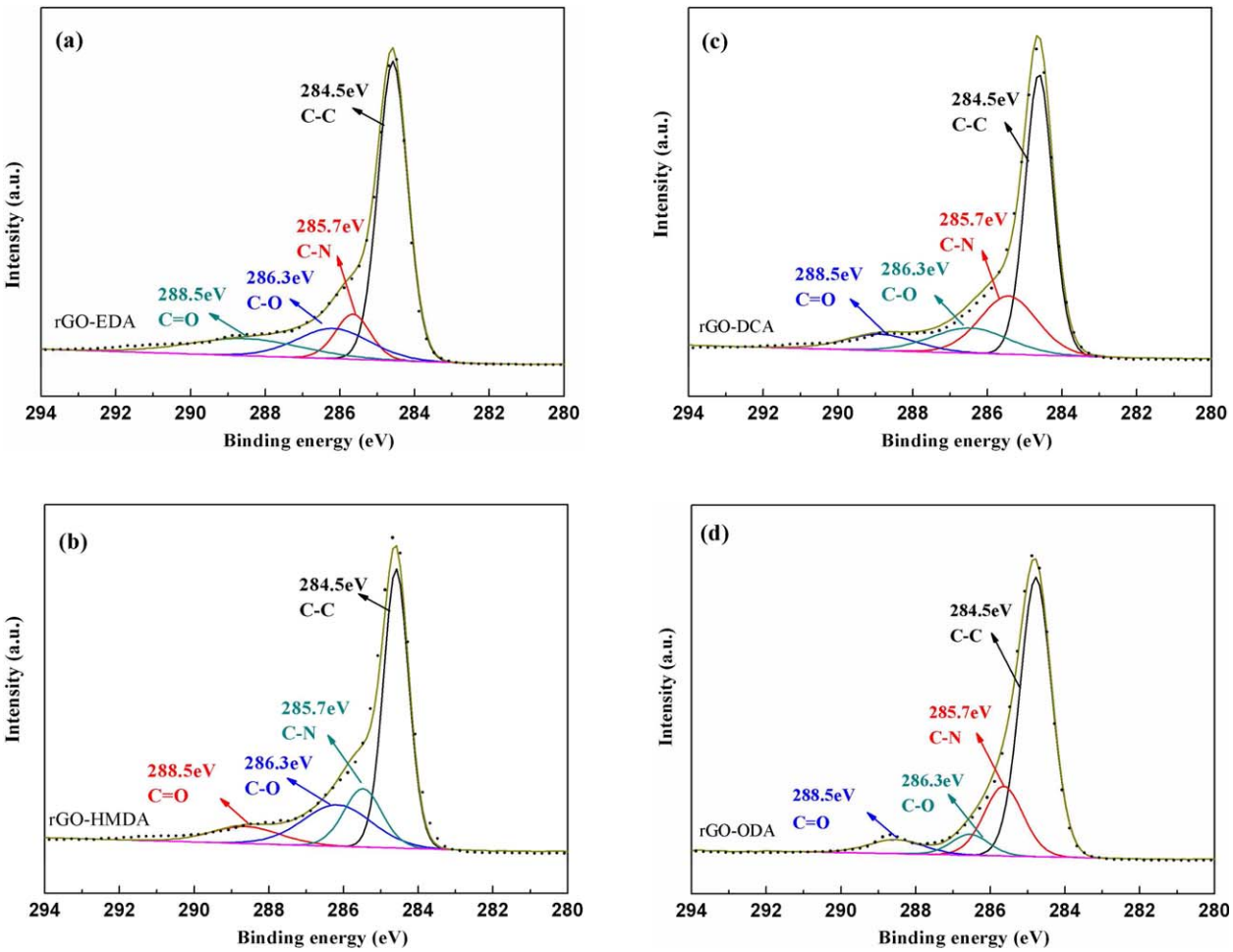

Figure 4. C1s XPS spectra of RAGOs, (a) rGO-EDA, (b) rGO-HMDA, (c) rGO-DCA, and (d) rGO-ODA. [Color figure can be viewed in the online issue, which is available at wileyonlinelibrary.com.]

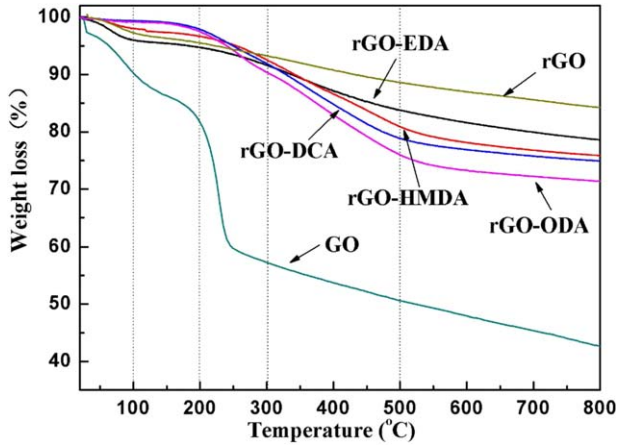

Figure 5. TGA curves of GO, rGO, and RAGOs. [Color figure can be viewed in the online issue, which is available at wileyonlinelibrary.com.]

successful grafting of amines to the surface of GO, and the successful reduction by $N_2H_4 \cdot H_2O$, resulting in an enhancement of hydrophobicity. Substantially, the weight loss decreased with the increasing of the length of amine chains (rGO-DCA < rGO-ODA < rGO-HMDA < rGO-EDA) below about 220 °C. At this stage, the weight loss could be contributed to two parts. The first part was the thermal decomposition of the small quantity of residual oxygen-containing groups on the surface of RAGOs; the second part could be the thermal degradation of the grafted amine moieties. The thermal decomposition occurred in the range of 300–500 °C could mainly correspond to the degradation of amine moieties covalently linked on the surface of GO. Furthermore, it was noteworthy that in this temperature range, the weight loss increased with the increasing of the length of amine chains (rGO-EDA < rGO-HMDA < rGO-DCA < rGO-ODA). This was associated with the length of chains on one hand, the amines with shorter chain length obtained smaller weight mass, it caused less weight loss in this stage; while on the other hand, there were two amine groups on the end of the chains for EDA and HMDA but only one for DCA and ODA. The diamines could form more covalent bond than monoamines, resulting in the better thermal stability. The final residual weight at 800 °C were 78.55, 75.81, 74.88, and 71.27% for rGO-EDA, rGO-HMDA, rGO-DCA, and rGO-ODA, respectively, which were much higher than that of GO (42.49%). While in comparison with rGO (84.22%), the residual weights of rGO-EDA, rGO-HMDA, rGO-DCA, and rGO-ODA were slightly lower at 800 °C, it was due to the thermal decomposition of grafted amine chains. It indicated the successful functionalization and grafting of amine chains. The TGA results showed that RAGOs had much better thermal stability than pristine GO due to the removal of oxygen-containing groups by the reduction of $N_2H_4 \cdot H_2O$ and indicated the successful grafting of amine chains.

Table II. TGA Results of GO and RAGOs

	Residual weight (%)				
Samples	100 °C	200 °C	300 °C	500 °C	800 °C
GO	90.26	81.72	57.27	50.63	42.49
rGO	97.28	95.48	93.23	88.57	84.22
rGO-EDA	96.27	94.70	91.63	83.77	78.55
rGO-HMDA	98.05	96.63	92.50	80.85	75.81
rGO-DCA	99.41	97.82	91.91	78.87	74.88
rGO-ODA	99.18	97.44	90.37	75.62	71.27

Morphology of RAGOS/PI Composites

In order to study the interfacial interactions between RAGOs and the PI matrix, SEM images of the fractured surfaces of the RAGOs/PI composites were used to observe the dispersion of RAGOs in the matrix. Figure 6 showed the SEM images of different samples at different magnification times.

For the neat PI [Figure 6(a)], the fractured surfaces were rather flat and smooth. In comparison with neat PI, the fractured surfaces of RAGOs/PI composites were relative rough. Furthermore, no obvious aggregation of the RAGOs was observed. It indicated the good dispersion of RAGOs in the matrix. Moreover, RAGOs grafted with different amines showed different fractured surfaces. The rGO-EDA/PI and rGO-HMDA/PI showed similar fracture structure, the pull out of some PI matrix could be observed [Figure 6(b,c)]. This may be attributed to the reason that the diamine could link to the polymer chain and graphene because of the existence of more than one amine groups at the same time, resulting in formation of strong adhesion between the graphene and the polymer chain, the PI matrix and RAGOs may be pulled out together as a whole. Moreover, the existence of more than one amine groups could also link to different graphene and linked them together, and the amine chain was not long enough, so that the effect of restraining aggregation was limited, the re-aggregation of some RAGOs occurred. Some defects were produced because of that, the RAGOs and PI matrix were pulled out together as a whole, it generated holes in the composites. While for rGO-DCA/PI and rGO-ODA/PI composites [Figure 6(d,e)], it showed more homogenous dispersion. The monoamine was covalently linked to the surface of graphene and relative long chains had better effect of restraining restack of graphene. Furthermore, rGO-EDA and rGO-HMDA had relative shorter amines chain lengths, the polymer chains could intercalate the interlayers of graphene more easily during the *in situ* polymerization process. It formed strong interfacial interactions between the matrix and RAGOs with relative longer chain lengths, due to its longer chain lengths and contact area. The homogenous dispersion and strong interfacial interactions could favor the transfer of stress along the interface.

Mechanical Properties of RAGOS/PI Composites

The introduction of RAGOs showed significant enhancement on the mechanical properties of PI matrix. The tensile strength, tensile modulus, and elongation at break of RAGOs/PI with various loadings of RAGOs were shown in Figure 7.

From Figure 7(a,b) it could be seen that the tensile strength and tensile modulus increased dramatically with increase of the RAGOs content from 0 to 0.5 wt % at the first stage, then it increased slightly or even decreased with the increase of RAGOs content at the second stage. It could be attributed to the reason

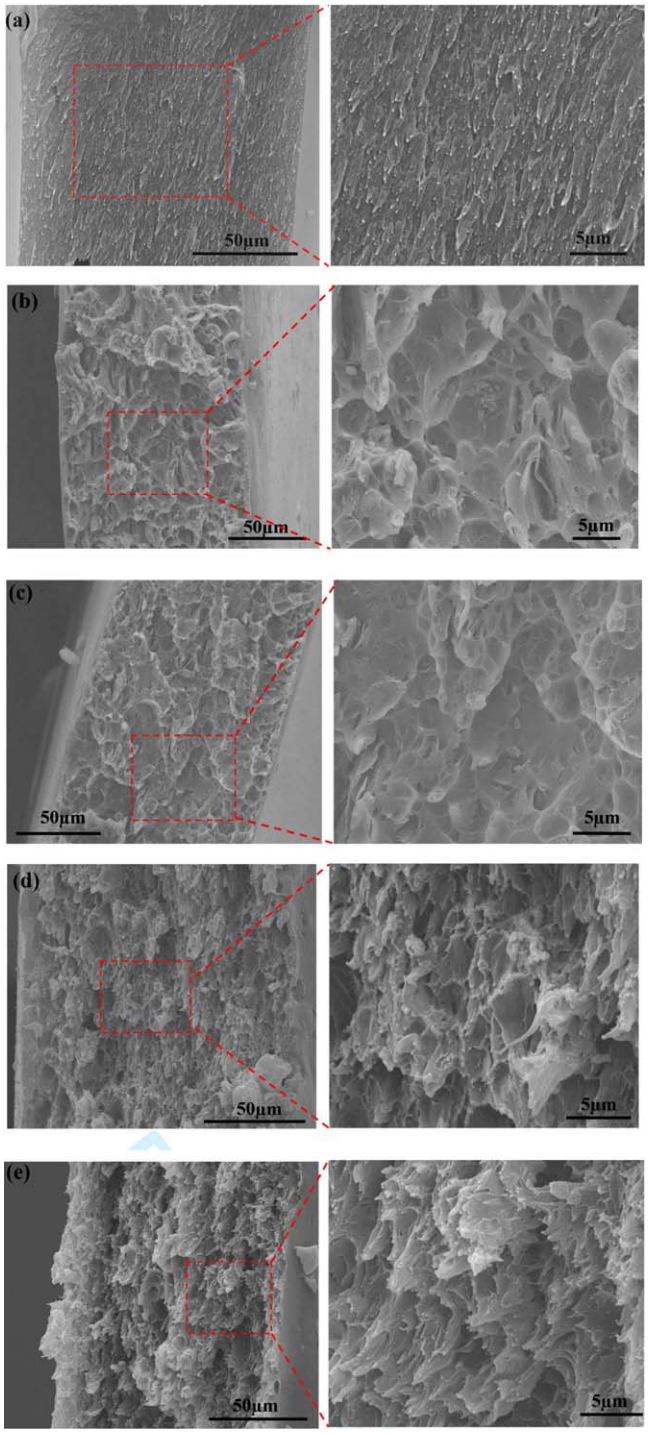

Figure 6. SEM images of cross sectional structure of (a) pure PI, (b) 0.5 wt % rGO-EDA/PI, (c) 0.5 wt % rGO-HMDA/PI, (d) 0.5 wt % rGO-DCA/PI, and (e) 0.5 wt % rGO-ODA/PI composites after tensile testing. [Color figure can be viewed in the online issue, which is available at wileyonlinelibrary.com.]

that when the RAGOs arrived at a critical content, the distance between the RAGOs sheets was very small, the adjacent RAGOs sheets tended to re-aggregate due to the effect of Van der Waals forces, resulting in the reducing of the reinforcing efficiency. From the results of electrical conductivity (Figure 8), a similar phenomenon could be found. The electrical conductivity increase no more with the increase of RAGOs content when the filler content reached 0.5 wt %. It indicated the network of RAGOs had been formed and further addition of the filler may

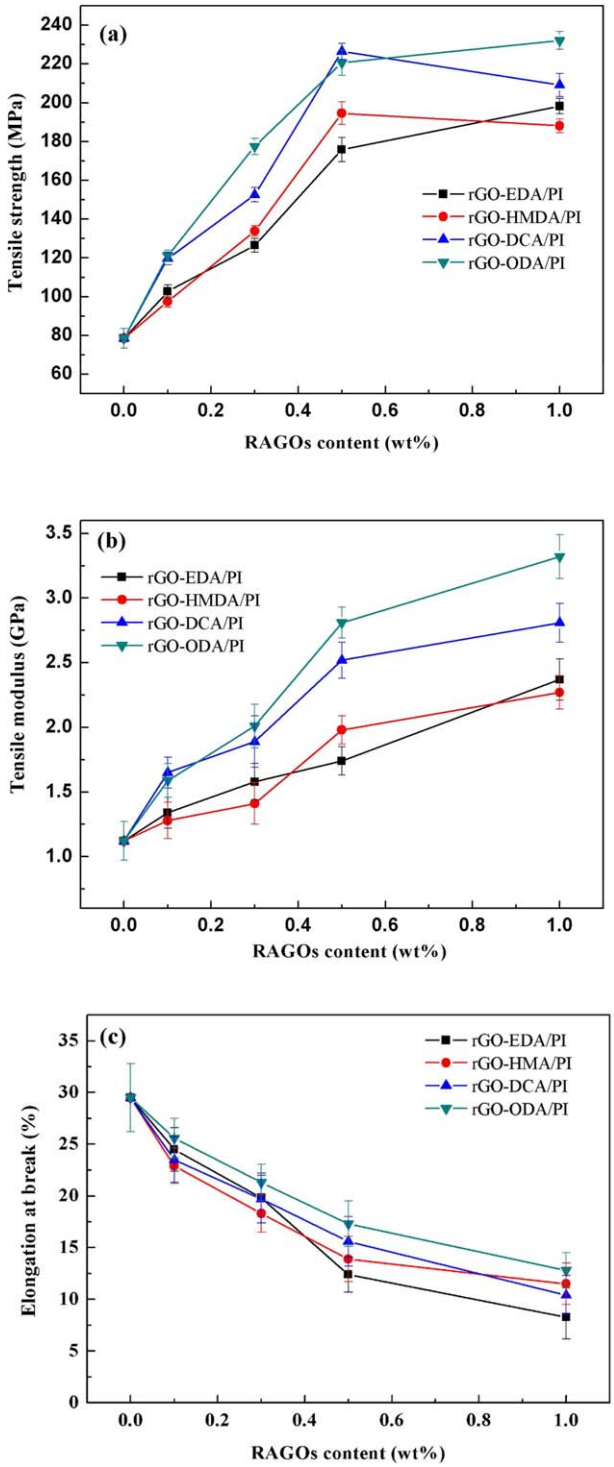

Figure 7. Variation of (a) tensile strength, (b) tensile modulus, and (c) elongation at break of RAGOs/PI composites, at different loadings of RAGOs. [Color figure can be viewed in the online issue, which is available at wileyonlinelibrary.com.]

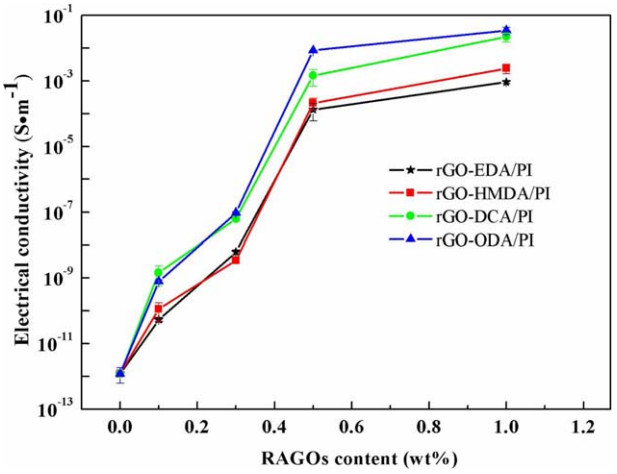

Figure 8. Electrical conductivity of RAGOs/PI composites. [Color figure can be viewed in the online issue, which is available at wileyonlinelibrary.com.]

cause re-aggregation of the fillers. What's more, from the SEM results in Figure 6, slight re-aggregation could be observed [Figure 6(e), for example], which indicated the further addition of the fillers would cause some restack of RAGOs and form defects. The formation of some small defects could not transfer the load efficiently, resulting in the limited reinforcement effect. When the content of RAGOs was 0.5%, the tensile strength and tensile modulus increased from 78.5 MPa and 1.12 GPa (neat PI) to 175.8 MPa, 194.6 MPa, 226.5 MPa, 220.7 MPa and 1.74 GPa, 1.98 GPa, 2.52 GPa and 2.81 GPa for rGO-EDA/PI, rGO-HMDA/PI, rGO-DCA/PI, and rGO-ODA/PI at 0.5 wt % RAGOs content, respectively. The tensile strength increased by 123.9, 147.9, 188.5, and 181.1% for rGO-EDA/PI, rGO-HMDA/PI, rGO-DCA/PI, and rGO-ODA/PI composites. And it was with 55.4, 76.8, 125.0, and 150.9% increase for the tensile modulus. The significant reinforcement effect was contributed to the superior homogenous dispersion of RAGOs in the polymer matrix and excellent compatibility of RAGOs and PI. The forming of strong interfacial interactions along the interface could promote the stress transferring efficiently. However, because rGO tended to re-aggregate, the forming of the defects in the composites would lead to rather limited enhancement effect. For example, the tensile strength of rGO/PI composites with 0.5 wt % rGO was only 117.2 MPa and it increased to 132.5 MPa when the addition content of rGO increased to 1.0 wt %, which showed much lower improvement in comparison with RAGOs, and it even decreased to 108.4 MPa when the addition content increased to 2.0 wt %. It showed rather limited enhancement effect in comparison with RAGOs. Figure 7(c) showed the elongation at break of the composites deceased with increase of the RAGOs content. Obviously, the incorporation of RAGOs restricted the movement of the polymer chains significantly, leading to the increase of brittleness of the FGO/PI composites.

It was noteworthy that even though the incorporation of RAGOs could improve the mechanical properties of PI, different RAGOs behaved differently. Generally, the RAGOs with longer chains had more excellent reinforcement effect. It obtained higher tensile strength and tensile modulus, while the lower decrease of elongation at break was obtained. It could be also attributed to the better dispersion in the PI matrix (illustrated in SEM images, Figure 6), and the restriction of polymer chain movement was not efficient as the shorter amine chains of RAGOs. In order words, relative longer chains had better effect on the restriction of the restack of RAGOs. A proper content of RAGOs was conducive to the enhancement of the mechanical properties of composites. Moreover, for rGO-EDA and rGO-HMDA, there may be more defects on the surface due to the existence of more amine groups reacting with GO, resulting in the lower pristine properties than that of rGO-DCA and rGO-ODA. It leading to lower reinforcement effect. The rGO-DCA and rGO-ODA was not only dispersed uniformly in the matrix due to its relative longer chains, but also existed fewer defects on their surfaces. As a result, they showed much more excellent enhancement effect on the properties of the composites.

Electrical Conductivity of the RAGOS/PI Composites

Pure PI is an insulating material holding an electrical conductivity of about 10^{-12} S/m. The introduction of RAGOs to the composites could cause excellent enhancement effect on the electrical conductivity, as shown in Figure 8. After the chemical reduction of GO, most of the oxygen-containing groups were removed (XPS results, Figures 4 and 5), which helped the effective recovery of sp^2 network of carbon from sp^3 network.[20] Furthermore, the homogenous dispersion would lead to the good connection of adjacent RAGOs, which favored the achievement of an effect conductive pathway, resulting in the enhancement on the electrical conductivity of the composites. The electrical conductivity increased with the increase of the RAGOs and finally reached 9.28×10^{-4}, 2.43×10^{-3}, 2.22×10^{-2}, and 3.45×10^{-2} S/m for the rGO-EDA/PI, rGO-HMDA/PI, rGO-DCA/PI, rGO-ODA/PI at 1.0 wt % RAGOs content, increased by 8, 9, 10, and 10 orders in comparison with that of neat PI, respectively. In comparison, rGO showed rather limited enhancement effect. For example, the electrical conductivity of rGO/PI composites was 1.41×10^{-10} S/m when rGO content was 0.5 wt %, and it increased to 2.48×10^{-6} S/m with 1.0 wt % rGO. While, with the increasing of rGO content, the electrical conductivity of the composites showed a rather stable platform, it showed 4.37×10^{-5} S/m when the content was 2.0 wt %. The main drawback was the re-aggregation of rGO and it also indicated that after modification by amine chains, the RAGOs showed more uniform dispersion in the composites, resulting in much better enhancement effect.

Interestingly, the composites with RAGOs modified by EDA and HMDA showed lower electrical conductivity than that by DCA and ODA. It was the reason that during the modification process, the linkage of EDA or HMDA to the surface of GO caused more defective parts in comparison with DCA and ODA. From the TGA results (see Figure 5), there were more EDA and HMDA grafted to the surface of GO in comparison with DCA and ODA, resulting in more defective parts and lower electrical conductivity. What's more, it was also related to the more homogenous dispersion of rGO-DCA and rGO-ODA than that of rGO-EDA and rGO-HMDA (see Figure 6). Besides, the electrical conductivity increased when the content of RAGOs were low due to some part of electric pathway was generated but

incomplete. Especially when the RAGOs content increase from 0.3 to 0.5 wt %, the electrical conductivity increased dramatically by about 5 orders, indicating the formation of total electric pathway and achieved a high electrical conductivity of the composites. While there was no obvious increase of the electrical conductivity with the further increase of the filler content, it indicated that on the basis of the complete electrical network, the further increase of RAGOs would not contribute the electrical conductivity any more.

CONCLUSIONS

In summary, GO was firstly prepared via Hummers method and then covalently modified by four different alkyl-amines (EDA, HMDA, DCA, and ODA), and afterward reduced by $N_2H_4 \cdot H_2O$ to remove most of the oxygen-containing groups to obtain RAGOs. The characterization results of FTIR, XPS, and TGA indicated the success of the above processes. RAGOs were introduced to PI via *in situ* polymerization to prepare composites. The RAGOs could achieve a homogenous dispersion in the matrix and form strong interfacial adhesion with the PI matrix, this helped the enhancement on properties of the composites. Different RAGOs showed different enhancement effects on the properties of the composites. Generally, the tensile strength of the composites increased with the chain lengths of amines grafted to RAGOs, it arrived at 175.8, 194.6, 226.5, and 220.7 for rGO-EDA/PI, rGO-HMDA/PI, rGO-DCA/PI, and rGO-ODA/PI at 0.5 wt % content, respectively. The electrical conductivity increased significantly by introduced of RAGOs, 9.28×10^{-4}, 2.43×10^{-3}, 2.22×10^{-2}, and 3.45×10^{-2} S/m for the rGO-EDA/PI, rGO-HMDA/PI, rGO-DCA/PI, and rGO-ODA/PI at 1.0 wt % RAGOs content were achieved. The enhancement effect at the same content behaved as: rGO-EDA < rGO-HMDA < rGO-DCA < rGO-ODA. Therefore, it could be found that RAGOs grafted by the amines with relative longer chains would restrict the restack more effectively and hold better compatibility with the matrix, the better enhancement effect on the properties of the composites was achieved.

REFERENCES

1. Sengupta, R.; Bhattacharya, M.; Bandyopadhyay, S.; Bhowmick, A. K. *Prog. Polym. Sci.* **2011**, *36*, 638.
2. Song, P.; Cao, Z.; Cai, Y.; Zhao, L.; Fang, Z.; Fu, S. *Polymer* **2011**, *52*, 4001.
3. Mittal, G.; Dhand, V.; Rhee, K. Y.; Park, S. J.; Lee, W. R. *J. Ind. Eng. Chem.* **2015**, *21*, 11.
4. Dhakate, S. R.; Subhedar, K. M.; Singh, B. P. *RSC Adv.* **2015**, *5*, 43036.
5. Du, J.; Cheng, H. M. *Macromol. Chem. Phys.* **2012**, *213*, 1060.
6. Yu, C. Z.; Li, D. L.; Wu, W. H.; Luo, C. Z.; Zhang, Y. P.; Pan, C. X. *J. Mater. Sci.* **2014**, *49*, 8311.
7. Lonkar, S. P.; Deshmukh, Y. S.; Abdala, A. A. *Nano Res.* **2015**, *8*, 1039.
8. Cano, M.; Khan, U.; Sainsbury, T.; O'Neill, A.; Wang, Z.; McGovern, I. T.; Maser, W. K.; Benito, A. M.; Coleman, J. N. *Carbon* **2013**, *52*, 363.
9. Kuila, T.; Khanra, P.; Mishra, A. K.; Kim, N. H.; Lee, J. H. *Polym. Test.* **2012**, *31*, 282.
10. Fim, F. D. C.; Basso, N. R.; Graebin, A. P.; Azambuja, D. S.; Galland, G. B. *J. Appl. Polym. Sci.* **2013**, *128*, 2630.
11. Chen, D.; Feng, H.; Li, J. *Chem. Rev.* **2012**, *112*, 6027.
12. Dai, J. F.; Wang, G. J.; Ma, L.; Wu, C. K. *J. Mater. Sci.* **2015**, *50*, 3895.
13. Huang, X.; Qi, X.; Boey, F.; Zhang, H. *Chem. Soc. Rev.* **2012**, *41*, 666.
14. Zhang, Y.; Mark, J. E.; Zhu, Y.; Ruoff, R. S.; Schaefer, D. W. *Polymer* **2014**, *55*, 5389.
15. Yang, K.; Huang, X. Y.; Fang, L. J.; He, J. L.; Jiang, P. K. *Nanoscale* **2014**, *24*, 14740.
16. Son, Y. R.; Rhee, K. Y.; Park, S. *J. Compos. Part B-Eng.* **2015**, *83*, 36.
17. Hummers, W. S.; Offeman, R. E. *J. Am. Chem. Soc.* **1958**, *80*, 1339.
18. Wu, C. K.; Wang, G. J.; Dai, J. F. *J. Mater. Sci.* **2013**, *48*, 3436.
19. Stankovich, S.; Dikin, D. A.; Piner, R. D.; Kohlhaas, K. A.; Kleinhammes, A.; Jia, Y. Y.; Wu, Y.; Nguyen, S. T.; Ruoff, R. S. *Carbon* **2007**, *45*, 1558.
20. Wang, G. X.; Yang, J.; Park, J.; Gou, X. L.; Wang, B.; Liu, H.; Yao, J. *J. Phys. Chem. C* **2008**, *112*, 8192.